Cell Mol Neurobiol (2016) 36:1241–1256
DOI 10.1007/s10571-015-0322-3

ORIGINAL RESEARCH

Hydroxysafflor Yellow A Attenuates Neuron Damage by Suppressing the Lipopolysaccharide-Induced TLR4 Pathway in Activated Microglial Cells

Yanni Lv[1] · Yisong Qian[2] · Aijun Ou-yang[1] · Longsheng Fu[1]

Received: 2 November 2015 / Accepted: 22 December 2015 / Published online: 11 January 2016

Abstract Microglia activation initiates a neurological deficit cascade that contributes to substantial neuronal damage and impairment following ischemia stroke. Toll-like receptor 4 (TLR4) has been demonstrated to play a critical role in this cascade. In the current study, we tested the hypothesis that hydroxysafflor yellow A (HSYA), an active ingredient extracted from Flos Carthami tinctorii, alleviated inflammatory damage, and mediated neurotrophic effects in neurons by inducing the TLR4 pathway in microglia. A non-contact Transwell co-culture system comprised microglia and neurons was treated with HSYA followed by a 1 mg/mL lipopolysaccharide (LPS) stimulation. The microglia were activated prior to neuronal apoptosis, which were induced by increasing TLR4 expression in the activated microglia. However, HSYA suppressed TLR4 expression in the activated microglia, resulting in less neuronal damage at the early stage of LPS stimulation. Western blot analysis and immunofluorescence indicated that dose-dependently HSYA down-regulated TLR4-induced downstream effectors myeloid differentiation factor 88 (MyD88), nuclear factor kappa b (NF-κB), and the mitogen-activated protein kinases (MAPK)-regulated proteins c-Jun NH2-terminal protein kinase (JNK), protein kinase (ERK) 1/2 (ERK1/2), p38 MAPK (p38), as well as the LPS-induced inflammatory cytokine release. However, HSYA up-regulated brain-derived neurotrophic factor (BDNF) expression. Our data suggest that HSYA could exert neurotrophic and anti-inflammatory functions in response to LPS stimulation by inhibiting TLR4 pathway-mediated signaling.

Keywords Hydroxysafflor yellow A · Toll-like receptor 4 · Neuroprotective effect · Microglia · Neurons · Co-culture system · Anti-inflammatory · Neurotrophic

Introduction

Microglia primarily act as the resident immune cell of the mammalian central nervous system (CNS) (Block et al. 2007). Over-activated microglia could induce detrimental neurotoxic effects to the CNS following arteriosclerosis and cerebral ischemia diseases (Chen et al. 2015). In the mature adult brain, resting-state microglia extend numerous 30–50 μm branches to sense and survey the environment. When the CNS suffers an injury, such as inflammation, ischemia, or trauma, the microglia may become activated. The resting microglia transform from a ramified morphology to the characteristic-activated amoeboid macrophage morphology (Kettenmann et al. 2011). Microglia were the primary immune cells that were activated in response to LPS-induced neuronal injury in the CNS (Bozic et al. 2015). The LPS-induced over-activated microglia are involved in the release of inflammatory factors, such as tumor necrosis factor-α (TNF-α), interleukin-1β (IL-1β), and nitric oxide (NO). Moreover, nuclear factor kappa b (NF-κB) and mitogen-activated protein kinase (MAPK) signaling pathways are believed to lead to an inflammatory reaction in the over-activated microglia, resulting in neuronal death and brain injury (Park et al. 2015). Brain-derived neurotrophic factor (BDNF) expression plays an important role in restoring the

✉ Yanni Lv
lvyanni@126.com

[1] Pharmacy Department, The First Affiliated Hospital of Nanchang University, Yongwai Street 17, Nanchang 330006, People's Republic of China

[2] Institute of Translational Medicine, Nanchang University, Nanchang 330001, People's Republic of China

brain following the inflammatory reactions after stroke, which are presumed to be the consequence of microglial activation (Doeppner et al. 2014).

The toll-like family of receptors have close correlation with innate immunity in the microglia (Song et al. 2011). Among the toll-like receptors, TLR4 is primarily expressed in the microglia in the brain and acts as the regulatory switch in initiating the immune response in the microglia. It has been reported that the activation of TLR4 in vitro resulted in the neuronal death and apoptosis, which was dependent on the presence of microglia (Lehnardt et al. 2003). However, the microglia isolated from the $TLR4^{-/-}$ mice did not exhibit an immune response against traumatic brain injury (Zhu et al. 2014). The results showed that the activation of TLR4 in vitro resulted in neuronal death and apoptosis, which was dependent on the presence of microglia. Here, a co-culture system of microglia and primary neurons was established, based on previous reports, to further elucidate the intervention mechanism of the drug. Simultaneously, myeloid differentiation factor 88 (MyD88), a critical adapter protein for TLR4, leads to the activation of downstream NF-κB, and the subsequent production of proinflammatory cytokines was investigated (Li et al. 2011; Wang et al. 2009). The NF-κB and MAPK signaling pathways and the levels of inflammatory cytokines were monitored to determine the effect of abnormal TLR4 expression in microglia. The effects of the microglia on the neurons focused on TLR4 expression and its signaling pathways.

Hydroxysafflor yellow A (HSYA) is the major active component from the Chinese herb Flos Carthami (Honghua). Previous studies have indicated that HSYA possesses various types of bioactivities, including oxygen-free radical scavenging, anti-inflammatory, and anti-apoptotic activities (Tian et al. 2008; Wu et al. 2012; Ji et al. 2009). In addition, studies have also shown that HSYA could significantly suppress inflammatory responses and inhibit neuroinflammation in microglia; the mechanisms included suppressing the expression of proinflammatory mediators, such as the NF-κB signaling pathway and p38 phosphorylation, and up-regulating the Janus kinase 2/Signal transducer and activator of transcription-3 pathway (Zhang et al. 2014b, c; Li et al. 2013). We have previously demonstrated that the protective effects of the HSYA target proteins against cerebral ischemia reperfusion injury are primarily through the innate immunity pathway (Lv et al. 2015). However, this was not sufficient to dissect the underlying molecular mechanisms of HSYA on nerve cells following neurological injury. Using a co-culture system for microglia and neurons, the cellular morphology and molecular mechanism were analyzed to interpret the neuroprotective effects of HSYA in the co-culture system.

Materials and Methods

Cortical Neuron Cultures

Cortical cells were obtained from embryonic day 18 pregnant mice. The cortical tissues were digested in 0.125 % trypsin for 15 min and stripped in Ca^{2+}/Mg^{2+}-free Hank's balanced salt solution. The solution was then dispersed through a 40-μm cell strainer, and the filtered cells were distributed into a poly-L-lysine-coated (Sigma, Chemical Co. St. Louis, MO, USA) culture plate containing 0.5 mL Neurobasal medium supplemented with 2 % B27 (Invitrogen, Carlsbad, USA). The culture density was adjusted to 5×10^5 cells/mL cells and maintained at 37 °C in humidified incubator with 5 % CO_2 and 95 % room air. The neurons that had been cultured for 7 days were subjected to the Transwell co-culture experiments. All of the neurons described in this paper are referred to as cortical neurons.

Microglial Cultures

The microglial cells were purchased from the Institute of Biochemistry and Cell Biology, SIBS, CAS, resource number: 3111C0001CCC000063. The microglial cells were cultured at a density of 1×10^5 cells/mL in DMEM medium with 10 % Fetal Bovine Serum. The medium was replaced on the next day and cultured at 37 °C in humidified incubator with 5 % CO_2 and 95 % room air.

Transwell Co-culture System for Microglia and Neurons

The Transwell co-culture system utilized the non-contact Transwell inserts, as previously described (Zhu et al. 2014). The neurons (1×10^5 cells/mL) were subcultured in a 24-well plate. The Transwells were positioned approximately 2 mm above the neurons in each well. The 0.4-μm pore size polyester membrane was precoated with poly-L-lysine. The microglia were grown on the top layer of the Transwells and were separated from the neurons in the well by the polyester membrane. The polyester membrane prevented cell–cell contact, but allowed the diffusion of soluble factors. The DMEM media with 10 % Fetal Bovine Serum for the microglia were discarded. The floating microglia were washed three times with Leibovitz's L-15 medium and subsequently cultured in a chemically defined serum-free medium (EF12) (Pardo et al. 1997). After 24 h of culture, glial-conditioned medium was collected (de Bernardo et al. 2003). Approximately, 3×10^5 floating microglia/mL were subcultured in glial-conditioned medium and then plated onto the top layer.

The difference between the densities of the subcultured microglia and the primary neurons on the plate must be carefully minimized. The culture medium for the co-culture system was DMEM medium with 10 % Fetal Bovine Serum. The co-culture system was subjected to experiments after 1 day of culture to allow for both cell adhesion and growth. Then, 1 mg/mL LPS (Sigma, St. Louis, MO, USA), HYSA, LPS plus HSYA or DMSO (Sigma, St. Louis, MO, USA) as a solvent control was added to the media below the Transwells.

Co-culture Groups

Twenty-four hour is commonly used to investigate the LPS-induced changes in microglia (Klintworth et al. 2009; Hines et al. 2013). The LPS-induced changes in the morphology of the microglia and neurons were complete within 24 h. In protocol 1, the co-culture systems were randomly divided into 8 groups ($n = 9$ for each group). The groups were treated with seven concentrations of HSYA for 24 h: 12, 25, 50, 100, 200, 400, and 800 μM, respectively. The media were removed after 24 h. The cytotoxicity in the microglia and neurons within each co-culture system were separately detected using a cytotoxicity assay. In protocol 2, the HSYA-treated group were incubated with 50 or 100 μM HSYA dissolved in dimethyl sulfoxide (DMSO) (Sigma, St. Louis, MO, USA) for 0.5 h prior to the LPS stimulation, while the control + vehicle group was treated with an equal volume of DMSO. One mg/mL LPS was added to the co-culture system and incubated for different amounts of time. The co-culture systems were randomly divided into 16 groups ($n = 9$ for each group): (1) control + vehicle group, (2) 50 or 100 μM HSYA only group, and (3–16) 1 mg/mL LPS plus vehicle or 50 μM or 100 μM HYSA at the corresponding time. At the representative incubated periods, the microglia and neurons from one representative plate of each group were separately subjected to confocal microscopy observations and densitometric analysis. The microglia in each group were collected and subjected to TLR4 detection by Western blot. The neurons in each group were collected and the number of apoptotic neurons was quantified by TUNEL staining. In protocol 3, the HSYA-treated group received HSYA 0.5 h before the LPS stimulation, while the control + vehicle group was treated with DMSO. One mg/mL LPS was added to the co-culture system and incubated for 24 h. The co-culture systems were randomly divided into six groups ($n = 9$ for each group): (1) control + vehicle group, (2) 50 μM HSYA only group, (3) 100 μM HSYA only group, (4) 1 mg/mL LPS for 24 h, (5) 1 mg/mL LPS + 50 μM HYSA for 24 h, and (6) 1 mg/mL LPS + 100 μM HYSA for 24 h. After incubation, nuclear and cytoplasmic proteins from microglia were extracted by Nuclear–Cytosol extraction kit (Applygen Technologies Inc, Beijing, China). Then, proteins from the cytosolic and the mitochondrial fraction were collected for detecting the release of NF-κB p65 and its phosphorylation. The proteins collected from cytosolic were subjected to detect IκBa and phosphorylated IκBa expression. In protocol 4, the HSYA-treated group received HSYA 0.5 h before the LPS stimulation, while the control + vehicle group was treated with DMSO. One mg/mL LPS was added to the co-culture system and incubated for 24 h. The co-culture systems were randomly divided into six groups ($n = 9$ for each group): (1) control + vehicle group, (2) 50 μM HSYA only group, (3) 100 μM HSYA only group, (4) 1 mg/mL LPS for 24 h, (5) 1 mg/mL LPS + 50 μM HYSA for 24 h, and (6) 1 mg/mL LPS + 100 μM HYSA for 24 h. The neurons were subjected to Western blots to detect the cleaved caspase-3 protein. The microglia were subjected to MyD88, NF-κB p65, and BDNF protein expression and immunofluorescence assays, and critical members that are regulated by MAPK include protein kinase (ERK) 1/2, p38 MAPK (p38), and c-Jun NH2-terminal protein kinase (JNK) Western blots.

Cytotoxicity Assay

Cell viability was evaluated by the 3-(4,5-dimethylthiazol-2-yl)-2,5-diphenyltetrazolium bromide (MTT) reduction assay. As described in protocol 1, after 24 h of incubation, the media were removed. The Transwell was removed from the neuron-enriched medium. The microglia and neurons in each group were separately analyzed using the cytotoxicity assay. The cells were incubated with 0.5 mg/mL of the MTT solution for 3 h at 37 °C in humidified incubator with 5 % CO_2 and 95 % room air. Then, the supernatant was removed and the formazan crystals were solubilized in DMSO and measured at 490 nm. Cell viability was expressed as a percentage, with the vehicle-treated cells set to 100 %.

TUNEL Staining

TUNEL staining was performed using the cell death detection kit (Roche, Basilea, Switzerland), according to manufacturer's instructions. As described in protocol 2, the neurons in each group were subjected to TUNEL staining. The neurons were washed with phosphate-buffered saline (PBS) and fixed in 4 % (w/v) triformol for 60 min. The fixed neurons were again washed with PBS and incubated in freshly prepared 0.1 % (w/v) Triton X-100 and 0.1 % (w/v) sodium citrate for 2 min on ice in the dark. The images of the TUNEL-stained plates were acquired with MetaMorph imaging software (Molecular Devices) using a Nikon epi-fluorescence microscope equipped with a

CoolSNAP-EZ CCD (charge-coupled-device) camera (photometrics). The number of TUNEL-positive apoptotic neurons on the plate from each group were counted using the MetaMorph imaging software.

Isolation of Cytoplasmic and Nuclear Protein

As described in protocol 3, cultured medium from plates were removed and microglia were detached with cold phosphate-bufferedsaline (PBS) and centrifuged at 1000 rpm for 5 min at 4 °C. Pellets were resuspended in 200 μL of cytosol extraction buffer A and incubated on ice for 10 min. Then 10 μL cytosol extraction buffer B was added and incubated on ice for 1 min and centrifuged at 1000 rpm for 5 min at 4 °C. The pellet contains crude nuclei. The supernatant was transferred to a new tube and further centrifuged at 12,000 rpm for 5 min at 4 °C. The supernatant is cytoplasmic proteins. The crude pellet was washed once with 100 μL cytosol extraction buffer A, spined for 5 min at 1000 rpm, and the supernatant was discarded. 50 μL of cold nuclear extraction buffer was added and incubated on ice for 30 min. Finally, samples were centrifuged at 12,000 rpm for 5 min at 4 °C and supernatants were collected as nuclear proteins.

Immunofluorescence Image Acquisition of Microglia and Skeleton Analysis

According to protocol 2, the Transwell was removed from the neuron-enriched medium and the microglia were separated from the neurons. The cultured microglia and neurons were separately washed with PBS (pH 7.4) and fixed with ice-cold ethanol for 10 min at 4 °C. Then the cells were separately permeabilized with 10 % normal goat serum, 3 % bovine serum albumin, and 0.1 % Triton X-100 inPBS for 1 h, and then incubated with the primary antibody for 48 h at 4 °C. After washing, cells separately were incubated overnight with the secondary antibody at 4 °C. The wash step was repeated, the nuclei of all cells were then washed and incubated with 4′,6-diamidino-2-phenylindole (DAPI, 1:500, Millipore) for 15 min at room temperature. Morphological alterations of microglia labeled with anti-CD11b (1:200, Abcam) or neurons labeled with mouse anti-NeuN (1:200, Millipore) were estimated as previously described (Kurpius et al. 2006) using the confocal images. Briefly, the particle measurement feature of Image J was used to automatically evaluate the circularity index of microglia or neuron, using the formula $CI = 4\pi$ (area/perimeter^2). A circularity index of 1.0 indicates a perfect circle. The microglia or neuron complexity and branch length were assessed by skeleton analysis using Image J software, as described previously (Morrison and Filosa 2013). Briefly, confocal images were converted to 8-bit format, followed by noise de-speckling to eliminate single-pixel background fluorescence. Then, images were converted to binary images, which were analyzed using Analyze Skeleton plugin to assess the number of microglia or neuron processes, number of branch endpoints and maximum branch length for each cell. These results were analyzed as average per frame.

Western Blot Analysis

According to protocol 2, the microglia treated with LPS or HSYA for 5, 10, 20, 40 min, 1, 12, and 24 h were subjected to Western blots to detect TLR4 expression. The microglial lysates were separated by centrifugation at 12,000 × *g* at 4 °C for 15 min. The supernatant was collected and protein concentrations were determined by the BCA assay. Samples containing 40 μg of proteins were analyzed by electrophoresis on 12 % SDS-polyacrylamide gels. Subsequently, the proteins were transferred onto PVDF membranes in a Tris-glycine transfer buffer. The membranes were blocked with 5 % nonfat dry milk for 2 h at room temperature and then incubated with a mouse anti-TLR4 antibody (1:400, Abcam, Massachusetts, USA). After the membrane was washed in TBST, it was incubated in the appropriate AP-conjugated secondary antibody (diluted 1:2000 in secondary antibody dilution buffer) for 1 h at 37 °C.

According to protocol 3 and 4, the neurons treated with vehicle, LPS, or HSYA for 24 h were subjected to Western blots to detect the cleaved caspase-3 protein. The electrophoresis procedure was the same as described above. The membrane was blocked with 5 % freshly prepared degreased milk-TBST for 2 h at room temperature and then incubated with the following primary antibodies overnight at 4 °C: mouse anti-cleaved caspase-3 (1:400, CST, St. Louis, USA) and anti-β-actin (1:1,000, CST, St. Louis, USA). The proteins from the cytosolic and the mitochondrial fraction were collected for detecting the release of NF-κB p65 and its phosphorylation. The proteins collected from cytosolic were subjected to detect IκBa and phosphorylated IκBa expression. The control + vehicle group and the groups treated with LPS or HSYA for 24 h were subjected to Western blots to analyze MyD88, BDNF, p65, p-p65, ERK1/2, p-ERK1/2, JNK, p-JNK, p38, and p-p38 expression. The membranes were blocked with 5 % freshly prepared degreased milk-TBST for 2 h at room temperature and then incubated with the following primary antibodies overnight at 4 °C: rabbit anti-MyD88 (1:500, Abcam), mouse anti-NF-κB p65 (1:1000, CST), mouse anti-NF-κB p-p65 (1:1000, CST), rabbit anti-IκBα (1:1000, SCBT), mouse anti-phosphorylated-IκBα (1:1000, SCBT), mouse BDNF (1: 400, Abcam), mouse anti-JNK (1:1000, CST), mouse anti-p-JNK (1:1000, CST), mouse anti-

ERK1/2 (1:1000, CST), mouse anti-p-ERK1/2 (1:1000, CST), mouse anti-ERK1/2 (1:1000, CST), mouse anti-p38 (1:1000, CST), mouse anti-p-p38 (1:1000, CST), and anti-β-actin (1:1,000, CST). After washing in TBST, all of the membranes were incubated with the appropriate HRP-conjugated secondary antibody for 50 min. The bands were visualized with enhanced chemiluminescence and the images were captured using a bio-Image Analysis System (Bio-Rad, Hercules, CA, USA).

Determination of the TNF-α, IL-1β, and NO Levels in the Cell Culture Supernatants by ELISA

According to protocol 3, the cell culture supernatants from the control + vehicle, 24 h LPS stimulation, and HSYA-treated groups were collected and centrifuged at 12,000×*g* for 15 min at 4 °C. The cytokine concentrations were evaluated using ELISA kits (R&D Systems, Minneapolis, MN, USA), according to the manufacturer's guidelines. The cellular cytokine concentrations were expressed as picograms per milliliter. The absorbance at 450 nm was measured and the protein concentrations were determined using standard curves of the recombinant TNF-α, IL-1β, or NO proteins generated on an ELISA reader (Model ELX800; BioTek, USA).

Statistical Analysis

All values are expressed as mean ± SD The differences between the groups were compared using a one-way ANOVA followed by Tukey's post hoc test. An unpaired Student's *t* test was used to compare the data between two groups. The levels of significance were set to $P < 0.05$ and $P < 0.01$.

Results

The Optimal Concentration of HSYA was Chosen

In the Transwell co-culture system, the two cell types could not contact each other, but could communicate with each other through permeable, secreted factors. The appropriate drug concentration for the co-culture system was chosen for the subsequent experiments. The MTT reduction assay was used to examine the viability of the two cell types after the HYSA incubation. To determine the optimal concentration of HSYA, 12, 25, 50, 100, 200, 400, or 800 μM HSYA were applied to individual wells of the co-culture system. As shown in Fig. 1, the administration of 200 μM HSYA significantly reduced the microglial viability to 92.12 % (92.12 ± 3.67, $P < 0.05$, Fig. 1) compared to the control + vehicle group (100.01 ± 5.24, Fig. 1), whereas

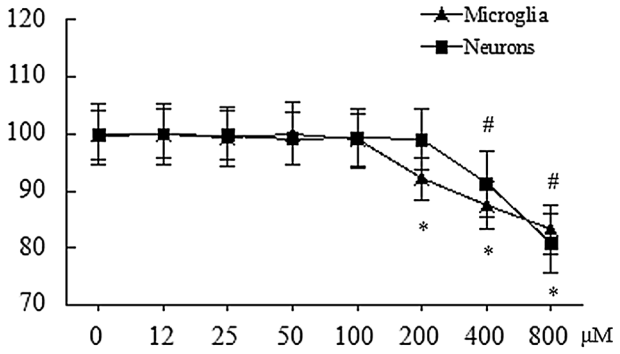

Fig. 1 12, 25, 50, 100, 200, 400, or 800 μM HSYA, respectively, were administered to the microglia and neurons in the co-culture system and incubated for 24 h. The cell viability of the neurons and microglia in the co-culture system was then detected using a cytotoxicity assay. The data are averages with SD, $n = 9$. $^{*}P < 0.05$ versus the control + vehicle group for microglial viability, $^{\#}P < 0.05$ versus the control + vehicle group for neuronal viability

the cell viability in the 12, 25, 50, and 100 μM HSYA-treated groups did not significantly differ from those in the control + vehicle group ($P < 0.05$, Fig. 1). Moreover, the administration of 400 μM (91.23 ± 5.69, $P < 0.05$, Fig. 1) and 800 μM (80.89 ± 5.21, $P < 0.05$, Fig. 1) HSYA significantly reduced the neuronal viability compared to the control + vehicle group (99.75 ± 4.24, Fig. 1). Low concentrations of HYSA were safe for both microglia and neurons. Taken together, 50 and 100 μM HSYA were chosen as the optimal concentration for the subsequent experiments.

The Morphological Changes of Microglia and Neurons were Observed

The LPS-induced morphological changes in microglia were described in the introduction. The resting-state microglia extend branches to survey the changes in the environment and neurons also sense the environmental changes with its branches. High-magnification confocal microscopy clearly demonstrated the morphological changes in the microglia and neurons from the different groups. Then, four monitoring indexes: circularity index, numbers of branches/cells, numbers of process endpoints/cell and maximum branch length (μm)/cells were applied to detect the morphological changes of microglia and neurons. The treatments with 50 or 100 μM HSYA for 24 h [circularity index (CI) 0.13 ± 0.05 and 0.14 ± 0.02, respectively, Fig. 2g] (numbers of branches 39.48 ± 3.05 and 40.56 ± 2.02, respectively, Fig. 2h) (numbers of process endpoints 9.45 ± 0.62 and 10.14 ± 1.07, respectively, Fig. 2i) (maximum branch length 20.56 ± 1.05 and 21.89 ± 2.02, respectively, Fig. 2j) did not affect the morphology of microglia and neurons compared with control + vehicle

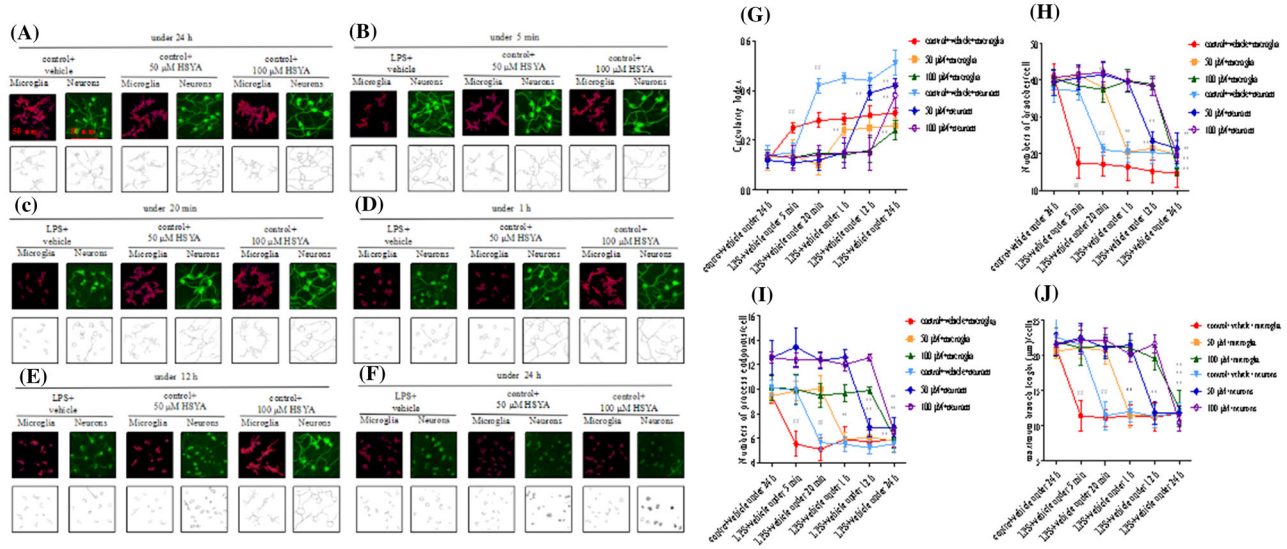

Fig. 2 The morphological changes and skeleton analysis in the neurons and microglia from the co-culture systems were observed under a confocal microscope. The co-culture system was stimulated with 1 mg/mL LPS or treated with 50 or 100 μM HSYA at different time points. HSYA was also administered 0.5 h before LPS stimulation and incubated with the co-culture system. *Bar* 50 μm. **a** Control + vehicle: skeleton analysis images of the morphology of the microglia or neurons from the control + vehicle group under 24 h; **b** skeleton analysis images of the morphology of the microglia or neurons treated with LPS or 50 or 100 μM HSYA under 5 min; **c** skeleton analysis images of the morphology of the microglia or neurons treated with LPS or 50 or 100 μM HSYA under 20 min; **d** skeleton analysis images of the morphology of the microglia or neurons treated with LPS or 50 or 100 μM HSYA under 1 h; **e** skeleton analysis images of the morphology of the microglia or neurons treated with LPS or 50 or 100 μM HSYA under 12 h; **f** skeleton analysis images of the morphology of the microglia or neurons treated with LPS or 50 or 100 μM HSYA under 24 h. **g** The circularity index monitoring for microglia and neurons; **h** number of branches per cell monitoring for microglia and neurons; **i** the number of process endpoints per cell monitoring for microglia and neurons; **j** the maximum branch length (μm) per cell monitoring for microglia and neurons. The data are averages with SD, $n = 9$. $^{\#}P < 0.05$, $^{\#\#}P < 0.01$ versus the control + vehicle group for microglial or neuronal reactivity indexes, $^{*}P < 0.05$, $^{**}P < 0.01$ versus microglial or neuronal reactivity indexes under the corresponding LPS stimulation time

groups at the corresponding incubation time (CI 0.12 ± 0.03 and 0.14 ± 0.04, respectively, Fig. 2g) (numbers of branches 37.45 ± 3.54 and 41.05 ± 3.56, Fig. 2h) (numbers of process endpoints 9.52 ± 0.67 and 10.12 ± 0.65, Fig. 2i) (maximum branch length 22.56 ± 2.51 and 21.08 ± 1.56, Fig. 2j). In order to simplify the comparison between images, we chose the control + vehicle groups at 24 h as the representative control + vehicle group for every groups for comparison. LPS-triggered cell morphology is one of the marks of cell activation and used to categorize different activation states (Kettenmann et al. 2011). After 5 min of LPS stimulation, the microglia reduced the complexity of their shape by retracting the branches into the cell body (CI 0.25 ± 0.02, $P < 0.01$, Fig. 2g) (numbers of branches 17.50 ± 4.12, $P < 0.01$, Fig. 2h) (numbers of process endpoints 5.64 ± 0.67, $P < 0.01$, Fig. 2i) (maximum branch length 11.45 ± 2.03, $P < 0.01$, Fig. 2j). The microglia showed more heterogeneous shapes, ranging from spindle-, rod- and -ramified shaped with short-thick processes to an more amoeboid-like morphology, with increasing LPS stimulation time. The cell bodies of most of the control neurons exhibited fusiform and ellipse shapes, with elongated, thickened branches connected in a network. While 5 min of LPS stimulation resulted in morphological changes in the microglia, the neurons did not exhibit significant morphological changes compared with control + vehicle groups. After 20 min of LPS stimulation, the cell bodies of the neurons began to shrink and the branched network began to disappear (CI 0.14 ± 0.04, $P < 0.01$, Fig. 2g) (numbers of branches 21.06 ± 1.54, $P < 0.01$, Fig. 2h) (numbers of process endpoints 5.51 ± 1.02, $P < 0.01$, Fig. 2i) (maximum branch length 11.45 ± 2.12, $P < 0.01$, Fig. 2j). These results indicate that the microglia and neurons were activated at different time points. Skeleton morphological analysis was subjected to further detect more subtle morphological changes compatible with cellar activation. The neurons in the co-culture system underwent apoptosis after the activation of the microglia. However, when the cells were treated with HSYA after LPS stimulation, the microglial and neuronal damage in the co-culture groups were less pronounced (Fig. 2c). Microglial activation were postponed to 1 h of LPS stimulation in the presence of 50 μM HSYA (CI 0.24 ± 0.02, $P < 0.01$, Fig. 2g) (numbers of branches 20.48 ± 1.67, $P < 0.01$, Fig. 2h) (numbers

of process endpoints 5.87 ± 0.64, $P < 0.01$, Fig. 2i) (maximum branch length 11.48 ± 1.67, $P < 0.01$, Fig. 2j), and 24 h of LPS stimulation in the presence of 100 μM HSYA (CI 0.24 ± 0.02, $P < 0.01$, Fig. 2g) (numbers of branches 16.48 ± 2.54, $P < 0.01$, Fig. 2h) (numbers of process endpoints 6.12 ± 0.94, $P < 0.01$, Fig. 2i) (maximum branch length 12.45 ± 2.54, $P < 0.01$, Fig. 2j). Meanwhile, the neurons maintained their shape and branched network for 12 or 24 h after LPS stimulation in the presence of 50 or 100 μM HSYA (CI 0.39 ± 0.03 and 0.15 ± 0.07, respectively, $P < 0.01$, Fig. 2g) (numbers of branches 23.45 ± 2.46 and 19.56 ± 1.68, respectively, $P < 0.01$, Fig. 2h) (numbers of process endpoints 6.87 ± 0.76 and 6.58 ± 0.31, respectively, $P < 0.01$, Fig. 2i) (maximum branch length 11.85 ± 1.62 and 10.47 ± 1.42, respectively, $P < 0.05$, Fig. 2j). The HSYA treatment could effectively inhibit the LPS-induced morphological changes in the microglia and neurons.

HSYA Functions by Inhibiting TLR4 Expression

LPS stimulation up-regulated TLR4 expression in the microglia after 5 min (1.51 ± 0.12, $P < 0.01$, Fig. 3a; 1.42 ± 0.13, $P < 0.01$, Fig. 3c) compared to the control + vehicle group (1.09 ± 0.23, Fig. 3a; 0.90 ± 0.25, Fig. 3c). The up-regulation of TLR4 continued for 10 min (1.63 ± 0.24, $P < 0.05$, Fig. 3a; 1.64 ± 0.27, $P < 0.05$, Fig. 3c), 20 min (1.89 ± 0.24, $P < 0.05$, Fig. 3a; 2.10 ± 0.08, $P < 0.01$, Fig. 3c), 40 min (2.47 ± 0.16, $P < 0.01$, Fig. 3a; 2.67 ± 0.14, $P < 0.05$, Fig. 3c), 1 h (2.98 ± 0.19, $P < 0.01$, Fig. 3a; 3.15 ± 0.17, $P < 0.01$, Fig. 3c), 12 h (3.56 ± 0.21, $P < 0.01$, Fig. 3A; 3.41 ± 0.24, $P < 0.01$, Fig. 3c), and 24 h (3.97 ± 0.17, $P < 0.01$, Fig. 3a; 3.56 ± 0.12, $P < 0.01$, Fig. 3c) of LPS stimulation compared to the groups exposed to LPS for 5 min, which had the same tendency with those data in Fig. 4a. Interestingly, HSYA-alone showed a increase trend in TLR4 expression, although no statistical significance was achieved. LPS-induced TLR4 expression gradually increased over time, up to 24 h, with the highest expression (3.97 ± 0.17, $P < 0.01$, Fig. 3a; 3.56 ± 0.12, $P < 0.01$, Fig. 3c) in the microglia. The neurons in the control + vehicle group had a normal cellular morphology and tightly packed neuronal networks (Fig. 2), and the numbers of apoptotic neurons after 5 and 10 min of LPS stimulation (7.32 ± 3.46; 6.31 ± 3.17, Fig. 3b; 6.22 ± 5.20; 5.83 ± 5.89, Fig. 3d) were similar to the levels of control + vehicle group (4.76 ± 4.19, Fig. 3b; 5.31 ± 3.12, Fig. 3d). The number of apoptotic neurons had increased after 20 min of LPS stimulation (26.46 ± 2.19, $P < 0.05$, Fig. 3b; 27.82 ± 6.67, $P < 0.01$, Fig. 3d) compared to the groups exposed to LPS for 5 min. However, the up-regulated TLR4 expression in microglia was significantly neutralized by HSYA. Fifty μM HSYA down-regulated the LPS-induced TLR4 expression after 5 min (1.24 ± 0.12, $P < 0.05$, Fig. 3a), 10 min (1.37 ± 0.12, $P < 0.05$, Fig. 3a), 20 min (1.52 ± 0.17, $P < 0.05$, Fig. 3a), 40 min (1.87 ± 0.23, $P < 0.05$, Fig. 3a), 1 h (1.98 ± 0.24, $P < 0.01$, Fig. 3a), 12 h (2.12 ± 0.25, $P < 0.01$, Fig. 3a), and 24 h (2.49 ± 0.26, $P < 0.01$, Fig. 3a). One hundred μM HSYA down-regulated the LPS-induced TLR4 expression after 5 min (1.11 ± 0.17, $P < 0.05$, Fig. 3a), 10 min (1.10 ± 0.15, $P < 0.05$, Fig. 3a), 20 min (1.63 ± 0.12, $P < 0.01$, Fig. 3a), 40 min (2.16 ± 0.29, $P < 0.01$, Fig. 3a), 1 h (2.25 ± 0.29, $P < 0.01$, Fig. 3a), 12 h (2.42 ± 0.29, $P < 0.01$, Fig. 3a), and 24 h (2.15 ± 0.35, $P < 0.01$, Fig. 3a). After 12 and 24 h of LPS stimulation, 50 μM HSYA could down-regulate TLR4 expression to similar levels; meanwhile, after 24 h of LPS stimulation, 100 μM HSYA significantly down-regulated TLR4 expression in microglia. Simultaneously, the numbers of apoptotic neurons were obviously decreased after 12 or 24 h of LPS stimulation in the presence of 50 or 100 μM HSYA with the highest numbers, respectively (45.16 ± 2.74, $P < 0.01$, 52.45 ± 5.16, $P < 0.01$, Fig. 3b; 10.14 ± 3.35; 32.58 ± 7.06, $P < 0.01$, Fig. 3d), which was delayed compared to the LPS-induced apoptosis. Thus, we predicted that HSYA might exert its neuroprotective functions by down-regulating TLR4 expression in microglia.

Cleaved Caspase-3 Expression was Investigated in Neurons

Because 50 or 100 μM HSYA significantly suppressed TLR4 expression after 24 h of LPS stimulation, we used these parameters to investigate the changes in the downstream effectors of TLR4. Western blots were also applied to detect the neuronal changes after 24 h of LPS stimulation. The levels of the cleaved caspase-3 protein in the neurons from the co-culture system were detected after 24 h of LPS stimulation. Cleaved caspase-3 is well known as an executioner protease of apoptosis following brain ischemia (Zhu et al. 2014). That is why detection of cleaved caspase-3 is an excellent marker for apoptosis in immunohistochemistry. The levels of cleaved caspase-3 in the neurons were significantly increased after 24 h of LPS stimulation (2.20 ± 0.13, $P < 0.01$, Fig. 4) compared to the control + vehicle group (1.01 ± 0.06, Fig. 4). HSYA significantly decreased the up-regulated cleaved caspase-3 levels in a dose-dependent manner (1.57 ± 0.10, $P < 0.01$; 1.25 ± 0.05, $P < 0.01$, Fig. 4), respectively, compared to the groups exposed to LPS for 24 h, which was consistent with the decrease in the numbers of apoptotic neurons.

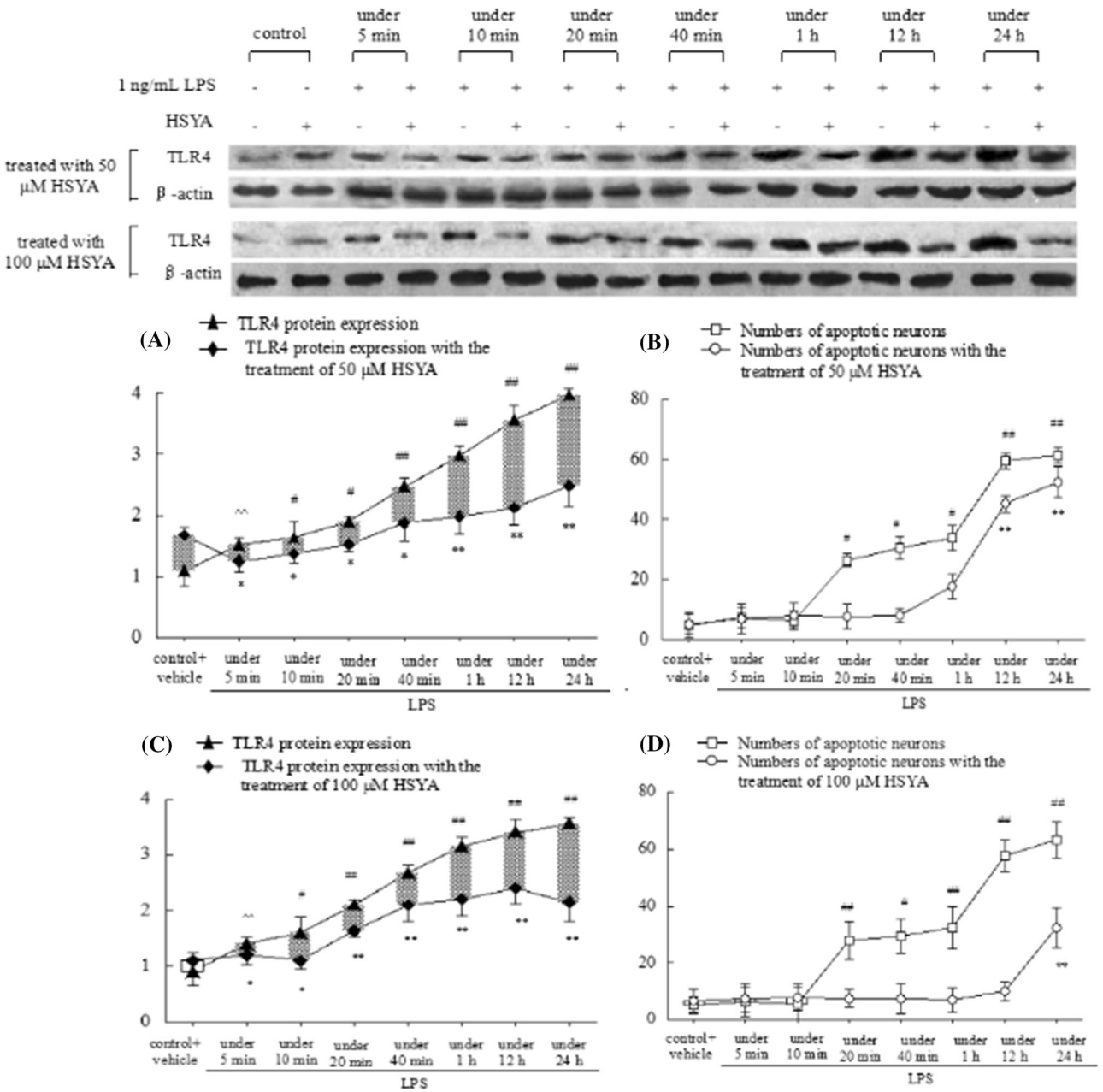

Fig. 3 The HSYA treatment up-regulated TLR4 expression in the microglia and reduced the numbers of apoptotic neurons in response to LPS. 50 or 100 μM HSYA were administered 0.5 h before the LPS stimulation. **a** The levels of the TLR4 protein in the stimulated microglia compared to 50 μM HSYA-treated groups at the corresponding time points. The data are averages with SD, $n = 9$. $^{\#}P < 0.05$, $^{\#\#}P < 0.01$ versus the control + vehicle group of microglia; $^{*}P < 0.05$, $^{**}P < 0.01$ versus the microglia after 5 min of LPS stimulation; **b** The numbers of apoptotic neurons in the LPS-stimulated group compared to 50 μM HSYA-treated groups at the corresponding time points. The data are averages with SD, $n = 9$. $^{\#}P < 0.05$, $^{\#\#}P < 0.01$ verus the control + vehicle group of neurons;$^{*}P < 0.05$, $^{**}P < 0.01$ versus the neurons after 5 min of LPS stimulation. **c** The levels of the TLR4 protein in the stimulated microglia compared to the 100 μM HSYA-treated groups at the corresponding time points. The data are averages with SD, $n = 9$. $^{\#}P < 0.05$, $^{\#\#}P < 0.01$ versus the control + vehicle group of microglia; $^{*}P < 0.05$, $^{**}P < 0.01$ versus the microglia after 5 min of LPS stimulation. **d** The numbers of apoptotic neurons in the stimulated microglia compared to the 100 μM HSYA-treated groups at the corresponding time points. The data are averages with SD, $n = 9$. $^{\#}P < 0.05$, $^{\#\#}P < 0.01$ versus the control + vehicle group of neurons; $^{*}P < 0.05$, $^{**}P < 0.01$ versus the neurons after 5 min of LPS stimulation

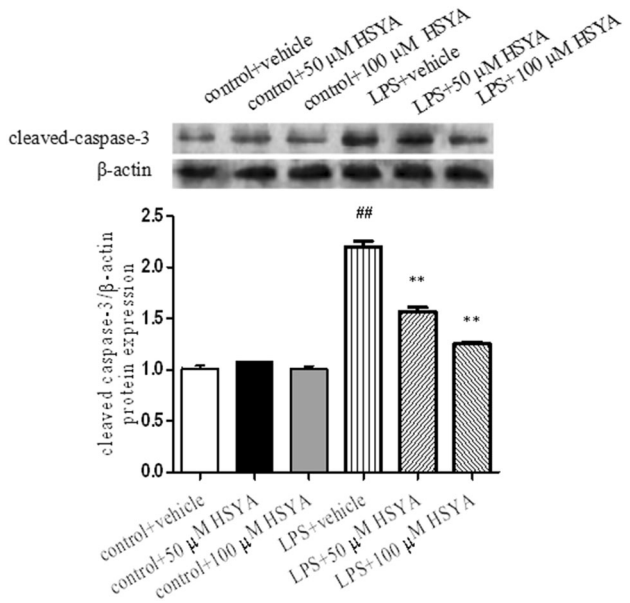

Fig. 4 Effects of 50 or 100 μM HSYA on the levels of the cleaved caspase-3 protein in the neurons after 24 h of 1 mg/mL LPS stimulation. The data are averages with SD, $n = 9$. $^{\#\#}P < 0.01$ versus the control + vehicle group for neurons, $^{*}P < 0.05$ versus neurons under 24 h of LPS stimulation. Control + vehicle: neurons in the control + vehicle group; control + 50 μM HSYA: neurons in the 50 μM HSYA-treated group; control + 100 μM HSYA: neurons in the 100 μM HSYA-treated group; LPS + vehicle: neurons in the LPS-treated group; LPS + 50 μM HSYA: neurons in the 50 μM HSYA plus LPS group; LPS + 100 μM HSYA: neurons in the 100 μM HSYA plus LPS group

HSYA Up-Regulated Brain-Derived Neurotrophic Factor (BDNF) Expression in the LPS-Stimulated Microglia

To further understand the effect of HSYA on TLR4 signaling in microglia, Western blots were performed to detect the expression of BDNF after 24 h of LPS stimulation. The levels of the BDNF protein in the microglia were decreased (0.73 ± 0.05, $P < 0.01$, Fig. 5a) after 24 h of LPS stimulation compared to the control + vehicle groups (1.01 ± 0.07, Fig. 5a). BDNF expression was not significantly different in the groups treated with 50 or 100 μM HSYA compared to the control + vehicle groups. Furthermore, BDNF expression was significantly up-regulated in the 50 μM HSYA- or 100 μM-treated groups compared to the groups exposed to LPS for 24 h (0.78 ± 0.02, $P < 0.01$; 0.90 ± 0.03, $P < 0.01$, respectively, Fig. 5a). The microglia were stained with an anti-CD11b antibody (green). The immunofluorescent staining demonstrated that 24 h of LPS stimulation weakened the intensity of the BDNF immunofluorescence intensity (red) compared to the control + vehicle group. Furthermore, the cells treated with 50 or 100 μM HSYA (604.50 ± 69.33, $P < 0.01$; 706.50 ± 21.17, $P < 0.01$, respectively, Fig. 5b, c) showed more robust BDNF immunofluorescence compared to the groups stimulated with LPS for 24 h (450.83 ± 33.05, Fig. 5b, c).

HSYA Inhibited MyD88 Expression and Decreased NF-κB p65 Expression, Phosphorylation, and Nuclear Translocation in the LPS-Stimulated Microglia

Western blots showed that MyD88 protein expression was increased dramatically in the LPS-stimulated microglia (2.32 ± 0.30, $P < 0.01$, Fig. 6) when compared with the control + vehicle groups (1.00 ± 0.08, $P < 0.01$, Fig. 6) and that it was significantly lower in 50 or 100 μM HSYA-treated mice than in LPS-stimulated microglia at 24 h (1.60 ± 0.06, $P < 0.01$, 1.42 ± 0.04, $P < 0.01$, Fig. 6). Protein extracts from cytosol and nuclei of microglia treated with vehicle or 50 or 100 μM followed by 24 h of LPS stimulation were subjected to a semiquantitative assessment. Western blots against p65 were performed. Results were expressed as nucleus/cytosol ratio. As shown in Fig. 7, LPS induced a remarkable increase in the translocation of p65 subunit (1.50 ± 0.08, $P < 0.01$, Fig. 7A), which was dose dependently decreased by HSYA treatment (1.32 ± 0.04, $P < 0.01$, 1.25 ± 0.03, $P < 0.01$, Fig. 7A). These results showed that HSYA was capable of inhibiting translocation of p65 subunit to the nucleus upon an inflammatory stimulus like LPS. Since degradation of IκBα proteins is an essential step for NF-κB activation, we further examined the effect of HSYA on the LPS-induced IκBα degradation. We found that IκBα phosphorylation had an increasing tendency in LPS-stimulated microglia (1.44 ± 0.03, $P < 0.01$, Fig. 7b). Dose-dependent HSYA could significantly inhibit IκBα phosphorylation by Western blot revealed the significant inhibitory effect on the LPS-induced IκBα phosphorylation in the presence of HSYA (1.35 ± 0.02, $P < 0.01$, 1.26 ± 0.02, $P < 0.01$, Fig. 7b). Western blots were also performed to detect the expression and phosphorylation of the NF-κB p65 after 24 h of LPS stimulation. The relative NF-κB p-p65/p65 protein levels in the microglia (2.52 ± 0.08, $P < 0.01$, Fig. 7c) were significantly increased after 24 h of LPS stimulation compared to the control + vehicle groups (0.78 ± 0.04, Fig. 7c). Furthermore, the relative NF-κB p-p65/p65 levels in the microglia were significantly down-regulated in the 50 μM or 100 μM HSYA-treated groups (2.15 ± 0.08, $P < 0.01$; 1.60 ± 0.06, $P < 0.01$, respectively, Fig. 7c). The immunofluorescence analysis also showed that the activated NF-κB p65 translocated to the nucleus and demonstrated the nuclear accumulation of NF-κB p65 in the microglia (1032.00 ± 39.96, $P < 0.01$, Fig. 7d, e). Pre-treatment with HSYA ameliorated these cellular localization changes, which were visible in the

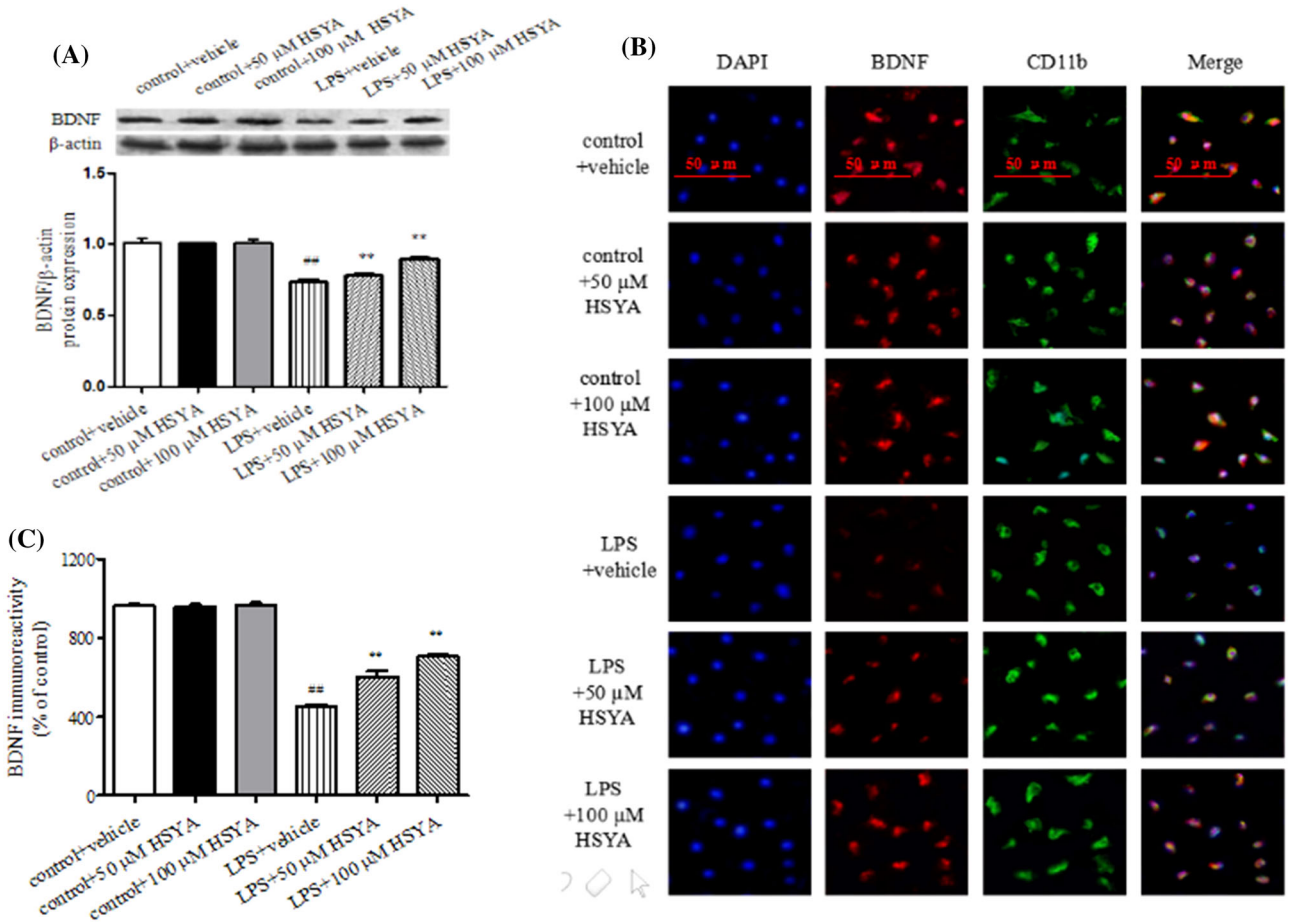

Fig. 5 Effects of HSYA on BDNF expression after 24 h of 1 mg/mL LPS stimulation, as detected by Western blots and immunofluorescence. **a** Effects of HSYA on BDNF expression in microglia after 24 h of 1 mg/mL LPS stimulation. **b** Effects of HSYA on the colocalization of CD11b and BDNF in the microglia. The BDNF was visualized by immunofluorescence staining (*red*) after 24 h; the cells were counterstained with DAPI (*blue*) and the microglia were stained with a CD11b antibody (*green*). *Bar* 50 μm. The images were captured under a confocal microscope with a magnification of ×200. The images are representative of nine individual plates from each group. **c** The immunoreactivity of BDNF in microglia localized in the Ganglion cell layer (GCL) was quantified. Results are expressed as percentage of control + vehicle from nine independent experiments. The data are averages with SD, $n = 9$. $^{\#\#}P < 0.05$ versus the control + vehicle group of microglia, $^{*}P < 0.05$ versus the microglia after 24 h of LPS stimulation. Control + vehicle: BDNF expression in the microglia from control + vehicle group; Control + 50 μM HSYA: BDNF expression in the microglia that were only treated with 50 μM HSYA; control + 100 μM HSYA: BDNF expression in the microglia that were only treated with 100 μM HSYA; LPS + vehicle: BDNF expression in the microglia that were only stimulated with LPS; LPS + 50 μM HSYA: BDNF expression in the microglia treated with 50 μM HSYA and LPS; LPS + 100 μM HSYA: BDNF expression in the microglia treated with 100 μM HSYA and LPS (Color figure online)

photomicrographs (811.50 ± 27.25, $P < 0.01$; 564.83 ± 44.75, $P < 0.01$, respectively, Fig. 7d, e).

HSYA Down-Regulated p-ERK1/2, p-JNK, and p-p38 Expression in the LPS-Stimulated Microglia

The LPS-stimulated microglia could induce the phosphorylation of the proteins in the MAPK signaling pathway, resulting in the production of inflammatory mediators. ERK1/2, JNK, and p38 are critical kinases of the MAPK family. The Western blot results showed that the relative levels of the p-ERK1/ERK1, p-ERK2/ERK2, p-JNK/JNK, and p-p38/p-38 (1.98 ± 0.01, $P < 0.01$, Fig. 8a; 1.31 ± 0.12, $P < 0.05$, Fig. 8a; 2.05 ± 0.01, $P < 0.05$, Fig. 8b; and 2.58 ± 0.10, $P < 0.01$, Fig. 8c, respectively) proteins were increased after 24 h of LPS stimulation compared to the control + vehicle groups (0.97 ± 0.16, Fig. 8a; 1.21 ± 0.19, Fig. 8a; 0.67 ± 0.05, Fig. 8b; and 1.16 ± 0.04, Fig. 8c, respectively). Dose-dependently HSYA decreased the LPS-induced up-regulation of p-ERK1/ERK1, p-JNK/JNK, and p-p38/p-38 (1.61 ± 0.09, $P < 0.01$, 1.45 ± 0.06, $P < 0.01$, Fig. 8a; 1.78 ± 0.04, $P < 0.01$, 1.65 ± 0.02, $P < 0.01$, Fig. 8b and 2.05 ± 0.15, $P < 0.01$, 1.83 ± 0.06, $P < 0.01$, Fig. 8c, respectively),

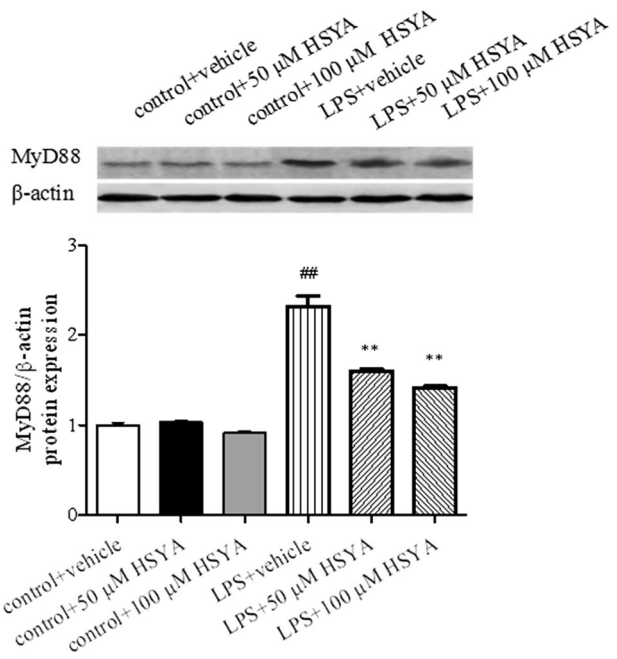

Fig. 6 Effects of 50 or 100 μM HSYA on the levels of the MyD88 protein in the neurons after 24 h of 1 mg/mL LPS stimulation. The data are averages with SD, $n = 9$. $^{\#\#}P < 0.01$ versus the control + vehicle group for microglia, $^{*}P < 0.05$ versus microglia under 24 h of LPS stimulation. Control + vehicle: neurons in the control + vehicle group; control + 50 μM HSYA: neurons in the 50 μM HSYA-treated group; control + 100 μM HSYA: neurons in the 100 μM HSYA-treated group; LPS + vehicle: neurons in the LPS-treated group; LPS + 50 μM HSYA: neurons in the 50 μM HSYA plus LPS group; LPS + 100 μM HSYA: neurons in the 100 μM HSYA plus LPS group

while had no effects on p-ERK2/ERK2 (1.24 ± 0.07, 1.21 ± 0.06, Fig. 8a).

HSYA-Attenuated Inflammatory Cytokines Release in the LPS-Stimulated Microglia

To identify the changes in the factors downstream of the NF-κB and MAPK pathways, the levels of the secreted cytokines after 24 h of LPS stimulation were examined by ELISA. The levels of TNF-α (129.46 ± 4.21, $P < 0.01$, Fig. 8d), IL-1β (157.47 ± 5.64, $P < 0.01$, Fig. 8d), and NO (69.46 ± 3.67, $P < 0.01$, Fig. 8d) secretion after 24 h of LPS stimulation were significantly increased compared to the control + vehicle group (TNF-α 40.12 ± 5.13), IL-1β (19.65 ± 3.68) and NO (27.96 ± 3.11) (Fig. 8d). However, 50 μM or 100 μM HSYA profoundly inhibited the LPS-induced up-regulation of TNF-α (110.26 ± 3.19, $P < 0.05$, 70.15 ± 5.64, $P < 0.01$, respectively), IL-1β (94.48 ± 3.17, $P < 0.01$, 63.24 ± 2.16, $P < 0.01$, respectively), and NO secretion (42.17 ± 2.56, $P < 0.05$, 35.01 ± 4.13, $P < 0.05$, respectively) (Fig. 8d).

Discussion

Microglia are activated by endogenous ligands to release a number of inflammatory cytokines, which have been demonstrated to play an important role in initiating cerebral ischemia reperfusion injury (Wang et al. 2014). Microglial cells fulfill the "double-edged sword" tasks within the CNS that are related to both the immune response and maintaining homeostasis (Jiang et al. 2014). Activated microglia use multiple mechanisms to secrete large amounts of cytokines (Zhang et al. 2015), matrix metalloproteinases (Lee et al. 2015a), and neurotoxic (Wu et al. 2015), BDNFs (Zhang et al. 2014a) to initiate the inflammatory cascade reaction. Therefore, therapeutic strategies targeting microglial activation are attractive approach to combat CNS injury.

The morphological changes in microglia and neurons in response to different periods of LPS stimulation were observed. Microglia are immune cells that scavenge the CNS for damage and can reflect environmental stimulation earlier than neurons (Nakajima and Kohsaka 2004). A time period of 24 h was sufficient to observe the morphological changes in the LPS-stimulated microglia. The LPS-induced morphological changes in the microglia and neurons were complete within 24 h. The up-regulation of circularity index and the down-regulation of numbers of branches, numbers of process endpoints, and maximum branch length presented that microglia morphology changed to a more amoeboid-like morphology. Meanwhile, under LPS stimulation, neurons shrink the cell bodies, circularity index were up-regulated and numbers of branches, numbers of process endpoints and maximum branch length were down-regulated. Five min of LPS stimulation resulted in the microglial activation, which was earlier than the neuronal apoptosis observed after 20 min of LPS stimulation. The increased number of microglia with an amoeboid shape represented the environmental changes in response to the neuronal damage in the CNS (Kraft and Harry 2011). As the LPS stimulation time increased, more microglia exhibited amoeboid shapes, which represented more severe inflammation in the CNS. Microglia are the defensive cells of the nervous system, and their activation is preceded by neuronal damage. The data proved once more that the neuronal changes were dependent on the presence of microglia. The increased TLR4 expression overtime was consistent with the time required for LPS-induced microglial activation. TLR4 had been shown to induce microglial activation and the release of inflammatory molecules that are responsible for the neurotoxicity observed in some CNS diseases (Lehnardt 2010). The inhibition of TLR4 expression in microglia may underlie the mechanism of neuroinflammation (Yao et al. 2013).

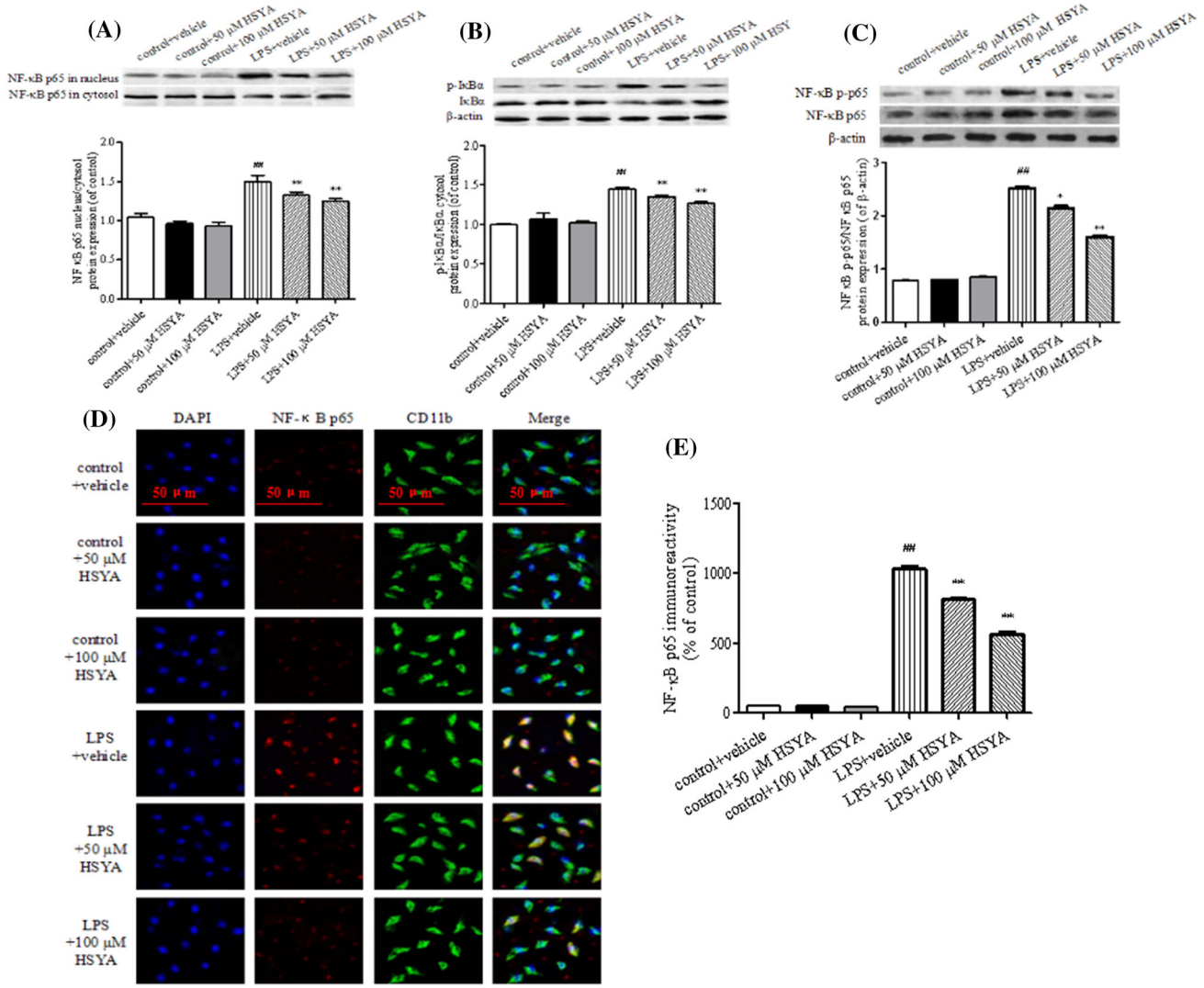

Fig. 7 Effects of HSYA on NF-κB p65 subunit translocation in the microglia after 24 h of 1 mg/mL LPS stimulation, as detected by Western blots and immunofluorescence. **a** Effect of HSYA on the degradation and phosphorylation of IκBα protein expression in cytosol of microglia treated with LPS for 24 h. **b** Effect of HSYA on the degradation and NF-κB p65 protein expression in nucleus/cytosol ratio of microglia treated with LPS for 24 h. **c** Effect of HSYA on the degradation and phosphorylation of NF-κB p65 protein expression in microglia treated with LPS for 24 h. **d** Effects of 100 μM HSYA on the colocalization of CD11b and NF-κB p65 in the microglia. NF-κB p65 was visualized by immunofluorescence staining (*red*) after 24 h of LPS stimulation; the cells were counterstained with DAPI (*blue*) and the microglia were stained with an CD11b antibody (*green*). *Bar* 50 μm. The images were captured under a confocal microscope with a magnification of ×200. The images are representative of six individual plates from each group. **e** The immunoreactivity of NF-κB p65 in microglia localized in the GCL was quantified. Results are expressed as percentage of control + vehicle from nine independent experiments. The data are averages with SD, $n = 9$. $^{\#\#}P < 0.05$ versus the control + vehicle group of microglia, $^{*}P < 0.05$ versus the microglia after 24 h of LPS stimulation. Control + vehicle: microglia from control + vehicle group; control + 50 μM HSYA: microglia that were only treated with 50 μM HSYA; control + 100 μM HSYA: microglia that were only treated with 100 μM HSYA; LPS + vehicle: microglia that were only stimulated with LPS; LPS + 50 μM HSYA: microglia treated with 50 μM HSYA and LPS; LPS + 100 μM HSYA: microglia treated with 100 μM HSYA and LPS (Color figure online)

HSYA is the active component in a traditional Chinese herb, which has been widely used in the clinic to treat cardiovascular and cerebral diseases. Preliminary experiments demonstrated that HSYA could effectively decrease the infarct volume and down-regulate TLR4 expression in a cerebral ischemia reperfusion mouse model (Chen et al. 2013). Furthermore, more detailed studies should focus on the mechanism in related cell models. Safe concentrations of HSYA were chosen via the MTT cytotoxicity assay. The results showed that 50 or 100 μM HSYA had no effect on the cellular morphology and downstream signaling molecules. In the presence of 50 or 100 μM HSYA, the microglia did not exhibit obvious morphological changes for 1 or 12 h after LPS stimulation. The administration of

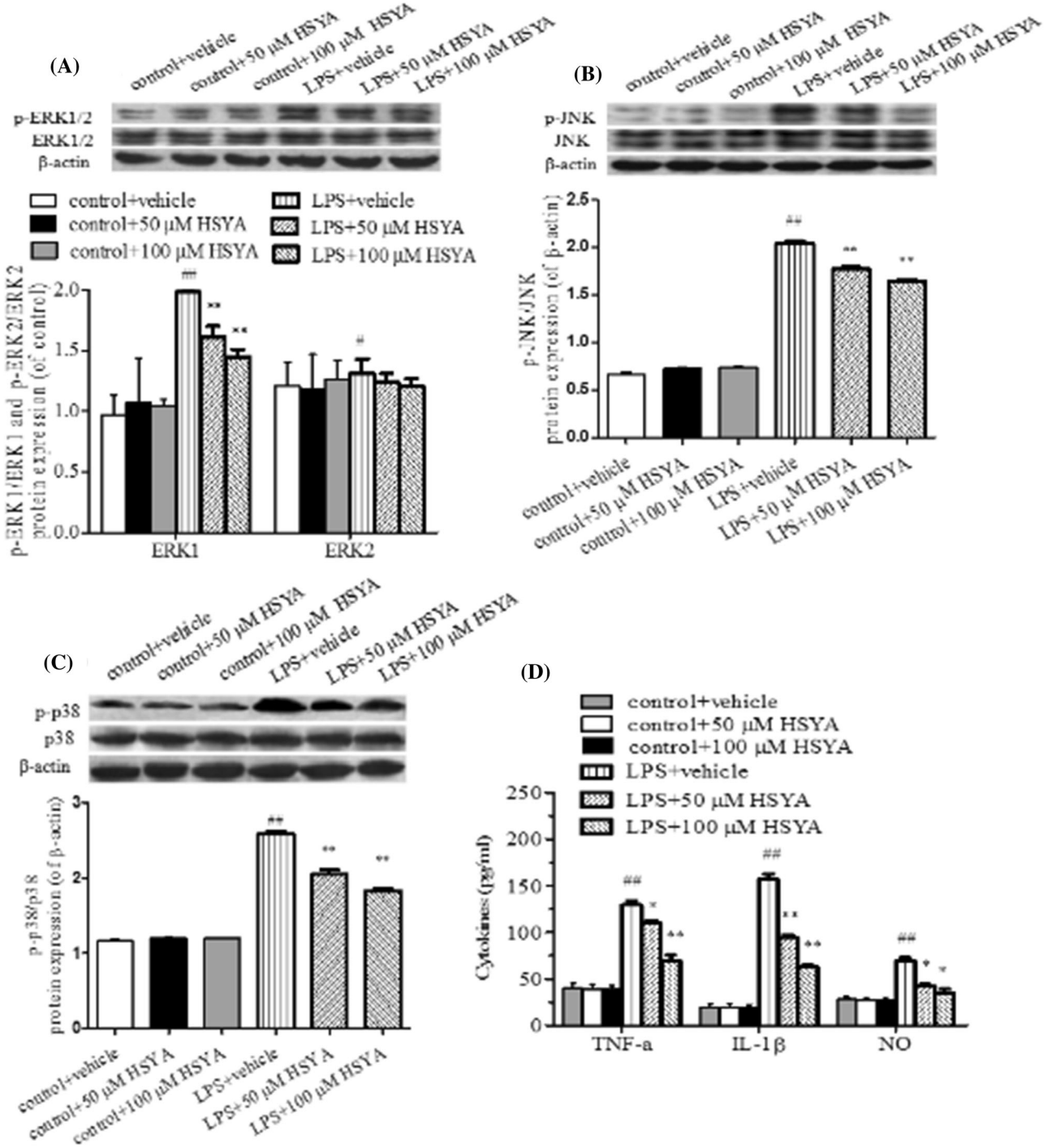

Fig. 8 Effects of HSYA on the ERK1/2, JNK, p38, and cytokine levels in the microglia after 24 h of 1 mg/mL LPS stimulation. **a** Effects of 100 μM HSYA on the relative levels of the ERK1/2 protein in microglia. **b** Effects of 100 μM HSYA on the relative levels of the JNK protein in microglia. **c** Effects of 100 μM HSYA on the relative levels of the p38 protein in microglia. **d** Effects of 100 μM HSYA on the TNF-α, IL-1β, and NO levels in microglia. The data are averages with SD, $n = 9$. $^{\#\#}P < 0.01$ versus the control + vehicle group of microglia, $^{\#}P < 0.05$ versus the control + vehicle group of microglia,$^{**}P < 0.05$ versus the microglia after 24 h of LPS stimulation, $^{*}P < 0.05$ versus the microglia after 24 h of LPS stimulation. Control + vehicle: ERK1/2, JNK, p38, or cytokine levels in the microglia from the control + vehicle group; control + 50 μM HSYA: ERK1/2, JNK, p38, or cytokine levels in the microglia that were only treated with 50 μM HSYA; control + 100 μM HSYA: ERK1/2, JNK, p38, or cytokine levels in the microglia that were only treated with 100 μM HSYA; LPS + vehicle: ERK1/2, JNK, p38, or cytokine levels in the microglia that were only stimulated with 1 mg/mL LPS; LPS + 50 μM HSYA: ERK1/2, JNK, p38, or cytokine levels in the microglia that were treated with 50 μM HSYA and LPS; LPS + 100 μM HSYA: ERK1/2, JNK, p38, or cytokine levels in the microglia that were treated with 100 μM HSYA and LPS

HSYA could prevent microglial alterations at the early stage of LPS-induced microglia reactivity. Meanwhile, in the presence of HSYA, the neurons exhibited the morphological changes of apoptosis after 12 or 24 h of LPS stimulation. In both the only-LPS stimulation condition or the LPS and HSYA condition, the activation times required for microglia were also later than those required for the neurons. Neuronal changes depend on the presence of microglia; thus, we inferred that HSYA could exert protective functions on neurons by inhibiting microglial activation. Microglia might be the therapeutic immune effectors for HSYA in treatments for CNS diseases. However, a more detailed molecular mechanism of the downstream signaling pathways needs to be investigated.

Upon activation of TLR4 signaling, the microglia undergo morphological changes and respond to pathogens by mediating immune responses through secreted signaling molecules. Microglia fulfill the 'double-edged sword' tasks, where beneficial effects are exerted through the release of neurotrophic factors. Among the neurotrophic factors, the BDNF supports neuronal survival and encourages the growth of new neurons and synapses (Song et al. 2014). LPS stimulation might cause a marked increase in BDNF mRNA expression (Chen et al. 2013). However, in the later, pathological process of inflammation stimulated by a high dose of LPS, BDNF was down-regulated, which, in turn, weakens its functions in neurons, leading to the aggravation of inflammation and injury (Umschweif et al. 2014; Lindvall et al. 1992; Tanaka et al. 2006). As shown in Fig. 6, we found that BDNF was down-regulated after 24 h of LPS stimulation compared to the control + vehicle group. Dose-dependently HSYA increased BDNF expression, thus inhibiting the LPS-induced down-regulation. The higher concentrations of HSYA up-regulated BDNF expression more than the lower concentration. However, the reports indicated that increasing BDNF might promote the cellular survival via inhibition of the caspase-3 pathway (Madeddu et al. 2004; Shulga et al. 2009; Kawamura et al. 2012), then the inhibition of caspase-3 pathway might be due to the up-regulation of BDNF expression. Thus, it is interesting to make further researches on whether BDNF in the microglia might influence the cleaved caspase-3 expression in neurons via non-contact co-culture system. These findings may indicate that HSYA might play a neuroprotective role by inducing the BDNF pathway.

In addition to its neurotrophic functions, within the TLR4 signaling pathway, the MyD88-dependent signaling pathway is an important activator of NF-κB and the subsequent regulatory effects of NF-κB signaling (Buchanan et al. 2010; Barton and Medzhitov 2003). Reports have indicated that TLR4/MyD88 cascade in microglia was essential for neuronal injury induced by HSP60 via the co-culture of WT neurons with MyD88$^{-/-}$ or Lps^{d} microglia (Lehnardt et al. 2008). Also, cerebral ischemia/reperfusion injury could be ameliorate through the down-regulation of TLR4/MyD88/TRAF6 signaling pathway via HMGB-1 inhibition in the treatment of Dioscin ameliorates (Tao et al. 2015). Here, the protein levels of MyD88 in microglia were increased by LPS, and HSYA attenuated the up-regulation of MyD88 in the TLR4 pathway. These data further indicate that HYSA regulates a complex series of inflammatory responses contributing to neuronal damage, in part through the microglial TLR4/MyD88 signaling pathway. TLR4 could activate a common signaling pathway by triggering NF-κB p65 expression and phosphorylation (Yoo et al. 2011). HSYA had been reported to inhibit the translocation of NF-κB p65 and IκB-α by inhibiting TLR4-mediated signaling following LPS-induced lung injury in mice (Sun et al. 2010). In accord with these reports, the levels and phosphorylation of NF-κB p65 were dose dependently decreased in response to the HSYA treatment. The MAPK pathway was also triggered after ischemia, and ERK1/2, JNK, and p38 phosphorylation were increased in the brains from normal mice (Lee et al. 2015b). Dose-dependently HSYA inhibited the phosphorylation of ERK1, JNK, and p38 in the LPS-stimulated microglia compared to the LPS only stimulation group. The TLR4 pathway also initiated neuroinflammatory cytokines via the NF-κB and MAPK pathways. The results showed the inflammatory cytokines downstream of TLR4, such as TNF-α, IL-1β, and NO, induced an inflammatory response (Prathab Balaji et al. 2015). One hundred μM HSYA had better neuroprotective effects on the cellular morphology and downstream signaling molecules than 50 μM HSYA. However, higher concentrations are cytotoxic in microglia. The therapeutic window for HSYA in the ischemia stroke requires careful consideration. Taken together, these data suggest that the protective effects of HSYA against inflammatory responses in microglia might be mediated through NF-κB/MAPK/cytokine signaling, which are targets of the TLR4 pathway.

The CD11b-positive cells were not exclusively microglia and also included monocytes and macrophages. The peripheral immune response might permit the monocytes or macrophages to infiltrate into the injured cells or tissues (Walker et al. 2012). However, the microglia were the focus of this paper. The inhibitory activities of HSYA on the microglia might also be due to the potential activation of monocytes or macrophages in response to LPS stimulation. The more precise molecular mechanism for these cell types is the focus of our future studies. TLR4 was tightly connected to the microglia in the CNS. However, TLR4 is widely expressed in neurons and astrocytes or related tissues in addition to in the microglia (Laflamme and Rivest 2001). TLR4 could participate in apoptosis of hippocampal neurons (He et al. 2013) or promote NF-

κB-dependent inflammatory response in astrocytes (Martorana et al. 2015). Still more, TLR4 played the critical role in astrocyte-microglia cooperation involved in the evolution of an inflammatory pathology on neurons (Barbierato et al. 2015). We study the TLR4 on a representative functional microglial-neuronal unit, while the effects of TLR4 in astrocytes on neurons or TLR4 functions in neuron itself was deserved further research.

Taken together, this study demonstrated that the HSYA treatment attenuated the TLR4 pathways in the LPS-stimulated microglia. The TLR4-induced innate immunity in microglia may be a candidate therapeutic target for clinical trials of cerebral ischemia injury diseases.

Compliance with Ethical Standards

Conflicts of Interest None of the authors declare conflicts of interest, including financial, personal, or other relationships with other individuals or organizations.

References

Barbierato M, Facci L, Argentini C, Marinelli C, Skaper SD, Giusti P (2015) Astrocyte-microglia cooperation in the expression of a pro-inflammatory phenotype. CNS Neurol Disord 201312(5):608–618

Barton GM, Medzhitov R (2003) Toll-like receptor signaling pathways. Science 300:1524–1525

Block ML, Zecca L, Hong JS (2007) Microglia-mediated neurotoxicity: uncovering the molecular mechanisms. Nat Rev Neurosci 8:57–69

Bozic I, Savic D, Laketa D, Bjelobaba I, Milenkovic I, Pekovic S, Nedeljkovic N, Lavrnja I (2015) Benfotiamine attenuates inflammatory response in LPS stimulated BV-2 microglia. PLoS One 10:e0118372

Buchanan MM, Hutchinson M, Watkins LR, Yin H (2010) Toll-like receptor 4 in CNS pathologies. J Neurochem 114:13–27

Chen L, Xiang Y, Kong L, Zhang X, Sun B, Wei X, Liu H (2013) Hydroxysafflor yellow A protects against cerebral ischemia-reperfusion injury by anti-apoptotic effect through PI3 K/Akt/GSK3β pathway in rat. Neurochem Res 38:2268–2275

Chen L, Yang Y, Li CT, Zhang SR, Zheng W, Wei EQ, Zhang LH (2015) CysLT2 receptor mediates lipopolysaccharide-induced microglial inflammation and consequent neurotoxicity in vitro. Brain Res 1624:433–445

de Bernardo S, Canals S, Casarejos MJ, Rodriguez-Martin E, Mena MA (2003) Glia-conditioned medium induces de novo synthesis of tyrosine hydroxylase and increases dopamine cell survival by differential signaling pathways. J Neurosci Res 73:818–830

Doeppner TR, Kaltwasser B, Teli MK, Bretschneider E, Bahr M, Hermann DM (2014) Effects of acute versus post-acute systemic delivery of neural progenitor cells on neurological recovery and brain remodeling after focal cerebral ischemia in mice. Cell Death Dis 5:e1386

He Y, Zhou A, Jiang W (2013) Toll-like receptor 4-mediated signaling participates in apoptosis of hippocampal neurons. Neural Regen Res 8:2744–2753

Hines DJ, Choi HB, Hines RM, Phillips AG, MacVicar BA (2013) Prevention of LPS-induced microglia activation, cytokine production and sickness behavior with TLR4 receptor interfering peptides. PLoS One 8:e60388

Ji DB, Zhang LY, Li CL, Ye J, Zhu HB (2009) Effect of Hydroxysafflor yellow A on human umbilical vein endothelial cells under hypoxia. Vascul Pharmacol 50:137–145

Jiang Z, Jiang JX, Zhang GX (2014) Macrophages: a double-edged sword in experimental autoimmune encephalomyelitis. Immunol Lett 160:17–22

Kawamura K, Kawamura N, Kawagoe Y, Kumagai J, Fujimoto T, Terada Y (2012) Suppression of hydatidiform molar growth by inhibiting endogenous brain-derived neurotrophic factor/tyrosine kinase B signaling. Endocrinology 153:3972–3981

Kettenmann H, Hanisch UK, Noda M, Verkhratsky A (2011) Physiology of microglia. Physiol Rev 91:461–553

Klintworth H, Garden G, Xia Z (2009) Rotenone and paraquat do not directly activate microglia or induce inflammatory cytokine release. Neurosci Lett 62:1–5

Kraft AD, Harry GJ (2011) Features of microglia and neuroinflammation relevant to environmental exposure and neurotoxicity. Int J Environ Res Public Health 8:2980–3018

Kurpius D, Wilson N, Fuller L, Hoffman A, Dailey ME (2006) Early activation, motility, and homing of neonatal microglia to injured neurons does not require protein synthesis. Glia 54:58–70

Laflamme N, Rivest S (2001) Toll-like receptor 4: the missing link of the cerebral innate immune response triggered by circulating gram-negative bacterial cell wall components. FASEB J 15:155–163

Lee EJ, Ko HM, Jeong YH, Park EM, Kim HS (2015a) β-Lapachone suppresses neuroinflammation by modulating the expression of cytokines and matrix metalloproteinases in activated microglia. Mol Neurodegener 10:61

Lee KM, Bang J, Kim BY, Lee IS, Han JS, Hwang BY, Jeon WK (2015b) Fructus mume alleviates chronic cerebral hypoperfusion-induced white matter and hippocampal damage via inhibition of inflammation and downregulation of TLR4 and p38 MAPK signaling. BMC Complement Altern Med 15:125

Lehnardt S (2010) Innate immunity and neuroinflammation in the CNS: the role of microglia in Toll-like receptor-mediated neuronal injury. Glia 58:253–263

Lehnardt S, Massillon L, Follett P, Jensen FE, Ratan R, Rosenberg PA, Volpe JJ, Vartanian T (2003) Activation of innate immunity in the CNS triggers neurodegeneration through a Toll-like receptor 4-dependent pathway. Proc Natl Acad Sci USA 100:8514–8519

Lehnardt S, Schott E, Trimbuch T, Laubisch D, Krueger C, Wulczyn G, Nitsch R, Weber JR (2008) A vicious cycle involving release of heat shock protein 60 from injured cells and activation of toll-like receptor 4 mediates neurodegeneration in the CNS. J Neurosci 28:2320–2331

Li GZ, Zhang Y, Zhao JB, Wu GJ, Su XF, Hang CH (2011) Expression of myeloid differentiation primary response protein 88 (Myd88) in the cerebral cortex after experimental traumatic brain injury in rats. Brain Res 1396:96–104

Li J, Zhang S, Lu M, Chen Z, Chen C, Han L, Zhang M, Xu Y (2013) Hydroxysafflor yellow A suppresses inflammatory responses of BV2 microglia after oxygen-glucose deprivation. Neurosci Lett 535:51–56

Lindvall O, Ernfors P, Bengzon J, Kokaia Z, Smith ML, Siesjö BK, Persson H (1992) Differential regulation of mRNAs for nerve growth factor, brain-derived neurotrophic factor, and neurotrophin 3 in the adult rat brain following cerebral ischemia and hypoglycemic coma. Proc Natl Acad Sci USA 89:648–652

Lv Y, Qian Y, Fu L, Chen X, Zhong H, Wei X (2015) Hydroxysafflor yellow A exerts neuroprotective effects in cerebral ischemia reperfusion-injured mice by suppressing the innate immune TLR4-inducing pathway. Eur J Pharmacol 769:324–332

Madeddu F, Naska S, Bozzi Y (2004) BDNF down-regulates the caspase 3 pathway in injured geniculo-cortical neurones. NeuroReport 15:2045–2049

Martorana F, Guidotti G, Brambilla L, Rossi D, Withaferin A (2015) Inhibits nuclear factor-κB-dependent pro-inflammatory and stress response pathways in the astrocytes. Neural Plast 2015:381964

Morrison HW, Filosa JA (2013) A quantitative spatiotemporal analysis of microglia morphology during ischemic stroke and reperfusion. J Neuroinflammation 10:4

Nakajima K, Kohsaka S (2004) Microglia: neuroprotective and neurotrophic cells in the central nervous system. Curr Drug Targets Cardiovasc Haematol Disord 4:65–84

Pardo B, Paino CL, Casarejos MJ, Mena MA (1997) Neuronal-enriched cultures from embryonic rat ventral mesencephalon for pharmacological studies of dopamine neurons. Brain Res Brain Res Protocol 1:127–132

Park J, Min JS, Kim B, Chae UB, Yun JW, Choi MS, Kong IK, Chang KT, Lee DS (2015) Mitochondrial ROS govern the LPS-induced pro-inflammatory response in microglia cells by regulating MAPK and NF-κB pathways. Neurosci Lett 584:191–196

Prathab Balaji S, Vijay Chand C, Justin A, Ramanathan M (2015) Telmisartan mediates anti-inflammatory and not cognitive function through PPAR-γ agonism via SARM and MyD88 signaling. Pharmacol Biochem Behav 137:60–68

Shulga A, Blaesse A, Kysenius K, Huttunen HJ, Tanhuanpää K, Saarma M, Rivera C (2009) Thyroxin regulates BDNF expression to promote survival of injured neurons. Mol Cell Neurosci 42:408–418

Song M, Jin J, Lim JE, Kou J, Pattanayak A, Rehman JA, Kim HD, Tahara K, Lalonde R, Fukuchi K (2011) TLR4 mutation reduces microglial activation, increases Aβ deposits and exacerbates cognitive deficits in a mouse model of Alzheimer's disease. J Neuroinflammation 8:92

Song J, Cheon SY, Jung W, Lee WT, Lee JE (2014) Resveratrol induces the expression of interleukin-10 and brain-derived neurotrophic factor in BV2 microglia under hypoxia. Int J Mol Sci 15:15512–15529

Sun CY, Pei CQ, Zang BX, Wang L, Jin M (2010) The ability of hydroxysafflor yellow a to attenuate lipopolysaccharide-induced pulmonary inflammatory injury in mice. Phytother Res 24:1788–1795

Tanaka S, Ide M, Shibutani T, Ohtaki H, Numazawa S, Shioda S, Yoshida T (2006) Lipopolysaccharide-induced microglial activation induces learning and memory deficits without neuronal celldeath in rats. J Neurosci Res 83:557–566

Tao X, Sun X, Yin L, Han X, Xu L, Qi Y, Xu Y, Li H, Lin Y, Liu K, Peng J (2015) Dioscin ameliorates cerebral ischemia/reperfusion injury through the downregulation of TLR4signaling via HMGB-1 inhibition. Free Radic Biol Med 84:103–115

Tian J, Li G, Liu Z, Fu F (2008) Hydroxysafflor yellow A inhibits rat brain mitochondrial permeability transition pores by a free radical scavenging action. Pharmacology 82:121–126

Umschweif G, Shabashov D, Alexandrovich AG, Trembovler V, Horowitz M, Shohami E (2014) Neuroprotection after traumatic brain injury in heat-acclimated mice involves induced neurogenesis and activation of angiotensin receptor type 2 signaling. J Cereb Blood Flow Metab 34:1381–1390

Walker PA, Shah SK, Jimenez F, Aroom KR, Harting MT, Cox CS Jr (2012) Bone marrow-derived stromal cell therapy for traumatic brain injury is neuroprotective via stimulation of non-neurologic organ systems. Surgery 152:790–793

Wang X, Stridh L, Li W, Dean J, Elmgren A, Gan L, Eriksson K, Hagberg H, Mallard C (2009) Lipopolysaccharide sensitizes neonatal hypoxic-ischemic brain injury in a MyD88-dependent manner. J Immunol 183:7471–7477

Wang W, Wang T, Feng WY, Wang ZY, Cheng MS, Wang YJ (2014) Ecdysterone protects gerbil brain from temporal global cerebral ischemia/reperfusion injury via preventing neuron apoptosis and deactivating astrocytes and microglia cells. Neurosci Res 81–82:21–29

Wu Y, Wang L, Jin M, Zang BX (2012) Hydroxysafflor yellow A alleviates early inflammatory response of bleomycin-induced mice lung injury. Biol Pharm Bull 35:515–522

Wu B, Huang Y, Braun AL, Tong Z, Zhao R, Li Y, Liu F, Zheng JC (2015) Glutaminase-containing microvesicles from HIV-1-infected macrophages and immune-activated microglia induce neurotoxicity. J Neuroinflammation 12:133

Yao L, Kan EM, Lu J, Hao A, Dheen ST, Kaur C, Ling EA (2013) Toll-like receptor 4 mediates microglial activation and production of inflammatory mediators in neonatal rat brain following hypoxia: role of TLR4 in hypoxic microglia. J Neuroinflammation 10:23

Yoo KY, Yoo DY, Hwang IK, Park JH, Lee CH, Choi JH, Kwon SH, Her S, Lee YL, Won MH (2011) Time-course alterations of Toll-like receptor 4 and NF-κB p65, and their co-expression in the gerbil hippocampal CA1 region after transient cerebral ischemia. Neurochem Res 36:2417–2426

Zhang X, Zeng L, Yu T, Xu Y, Pu S, Du D, Jiang W (2014a) Positive feedback loop of autocrine BDNF from microglia causes prolonged microglia activation. Cell Physiol Biochem 34:715–723

Zhang Z, Wu Z, Zhu X, Hui X, Pan J, Xu Y (2014b) Hydroxy-safflor yellow A inhibits neuroinflammation mediated by $A\beta_{1-42}$ in BV-2 cells. Neurosci Lett 562:39–44

Zhang ZH, Yu LJ, Hui XC, Wu ZZ, Yin KL, Yang H, Xu Y (2014c) Hydroxy-safflor yellow A attenuates $A\beta_{1-42}$-induced inflammation by modulating the JAK2/STAT3/NF-κB pathway. Brain Res 1563:72–80

Zhang L, Li YJ, Wu XY, Hong Z, Wei WS (2015) MicroRNA-181c negatively regulates the inflammatory response in oxygen-glucose-deprived microglia by targeting Toll-like receptor 4. J Neurochem 132:713–723

Zhu HT, Bian C, Yuan JC, Chu WH, Xiang X, Chen F, Wang CS, Feng H, Lin JK (2014) Curcumin attenuates acute inflammatory injury by inhibiting the TLR4/MyD88/NF-κB signaling pathway in experimental traumatic brain injury. J Neuroinflammation 11:59